Study on Process and Parameter Optimization of Selective Laser Sintering of Walnut Shell Composite Powder

Yueqiang Yu,[a] Yanling Guo,[a,c,]* Ting Jiang,[a] Jian Li,[a] Kaiyi Jiang,[b] and Hui Zhang [a]

This study aimed to improve the sintering quality of biomass composite powder by using walnut shell and copolyester hot melt adhesive (Co-PES) powders as the main raw materials to prepare the walnut shell/Co-PES composite (WSPC) powder for selective laser sintering (SLS). An orthogonal experimental design of five factors and four levels was adopted to optimize the process parameters for the SLS experiment. Moreover, through range analysis, the influences of laser power, preheating temperature, scanning speed, layer thickness, and scan spacing on the quality of WSPC were also studied. In addition, the synthesis weighted scoring method was used to determine the optimum process parameters. The results showed that the WSPC part quality was optimum when the laser power was 12 W, the scanning speed was 2000 mm/s, layer thickness was 0.15 mm, scan spacing was 0.2 mm, and preheating temperature was 80 °C.

Keywords: 3D printing; Biomass composite; Walnut shell powder; Orthogonal design; Synthesis evaluation

*Contact information: a: Northeast Forestry University, College of Mechanical and Electrical Engineering, Harbin, 150040, China; b: Northeast Forestry University, College of Engineering and Technology, Harbin, 150040, China; c: Northeast Forestry University, Research and Development Center of 3D Printing Material and Technology, Harbin, 150040, China; *Corresponding author: nefugyl@hotmail.com*

INTRODUCTION

Selective laser sintering (SLS) technology is a 3D printing technology (Deckard 1998). Unlike other 3D printing technologies, in the SLS process there is a wide material selection, no support is needed during manufacturing, and unsintered material could be recycled and reused (Jia *et al.* 2015). Therefore, SLS has been widely applied in industries such as the automotive, aerospace, casting parts, medical treatment, and construction industries (Mangano *et al*. 2013; Zhao *et al*. 2015b). For the sake of the present discussion, the term sintering will be understood to imply the localized melting and fusing together of particles that can include a hot-melt adhesive particles and walnut shell fragments.

With the development of SLS technology, the materials used in SLS play a decisive role in the sintering quality of sintered parts. Currently, materials for SLS mainly consist of metals, ceramics, polymers, and their corresponding composites (Stašić *et al*. 2014; Bai *et al*. 2016; Pace *et al*. 2017; Qi *et al*. 2017; Warnakula and Singamneni 2017). However, these materials lack structural diversity and cannot meet the demand of the market. Therefore, the authors developed a sustainable, low-cost, and environmentally friendly biomass composite as a new material for SLS. Previous research mainly focused on a single sintering experiment and forming process of composites from aspen wood, rice husk, and eucalyptus wood (Guo *et al*. 2011; Zeng *et al*. 2012a,b). With the in-depth study, the authors gained better efforts during the SLS experiment on composites from pine wood, bamboo, and walnut shell (Zhang *et al*. 2014; Zhao *et al.* 2015a; Yu *et al*. 2017). However, the SLS process of biomass composite powder comprises an extremely complex process of heat transfer and mass transfer. Although sintered parts of specific shape can be fabricated by SLS, there are some process defects such as warping deformation, layer-division, and over-sintering. A laser beam, as a direct heat source, radiates from biomass composite powder. Thus the quality of sintered parts not only depends on the interaction mechanism of the laser beam and biomass composite powder, but also depends on the process parameters of SLS. Hence, it is essential to study the influence of process parameters on the quality of the sintered biomass composite parts.

Walnut shell is a biomass material (Zheng *et al.* 2006). Compared to wood, rice husk, and bamboo, the walnut shell powder has unique advantages such as wide availability and ease of crushing. In addition, walnut shell powder of different particles diameters can be obtained without large and complex equipment, so that it is easy to meet the requirements of powder particle size of material by SLS. Walnut shell powder particle was approximately spherical. In SLS, an approximately spherical walnut shell powder particle is helpful for powder spreading and dispersing; the porous and good absorptive walnut shell particles are easily permeated with mixture liquid of molten Co-PES powder, which is the basis of producing forming precision, and mechanical properties of sintered parts. Therefore, in this research, walnut shell powder was used as the raw material to prepare WSPC powder. In addition, an orthogonal experimental design of five factors and four levels was adopted to discuss the influence rule of process parameters for SLS on the quality of the walnut shell/Co-PES composite (WSPC) parts.

EXPERIMENTAL

Materials

Equipment and process principle

The SLS experiments were conducted using an AFS-360 rapid prototyping instrument (Longyuan Technology Ltd., Beijing, China) equipped with a CO_2 laser generator (wavelength of 10.6 μm and laser power of 55 W). The dimensions of the forming box were 360 mm × 360 mm × 500 mm with a forming speed of 60 cm^3/h to 100 cm^3/h, a layer thickness range of 0.08 mm to 0.3 mm, and without any N_2 protection. The 3D entity objects were produced from a computer aided design model by the selective sintering of successive layers of powder. Powder under laser beam was fused to itself and to the preceding layer, in a repeated fashion. Rapid prototyping equipment and the schematic process diagram are shown in Fig. 1.

Preparation of WSPC powder

Walnut shell powder (approximately spherical particles of diameter range 58 μm to 96 μm, and an apparent density of 0.48 g/cm^3) was obtained from food enterprise (Ding Sheng Corundum Abrasives Ltd., Gongyi, China), as shown in Fig. 2(a). The copolyester hot melt adhesive (Co-PES) powder (smooth-surfaced white block particles of diameter range 0 μm to 58 μm, and apparent density of 0.7 g/cm^3) was provided by Tiannian Material Technology Ltd. (Shanghai, China), shown in Fig. 2(b). The light stabilizers and lubricants used were commercially available.

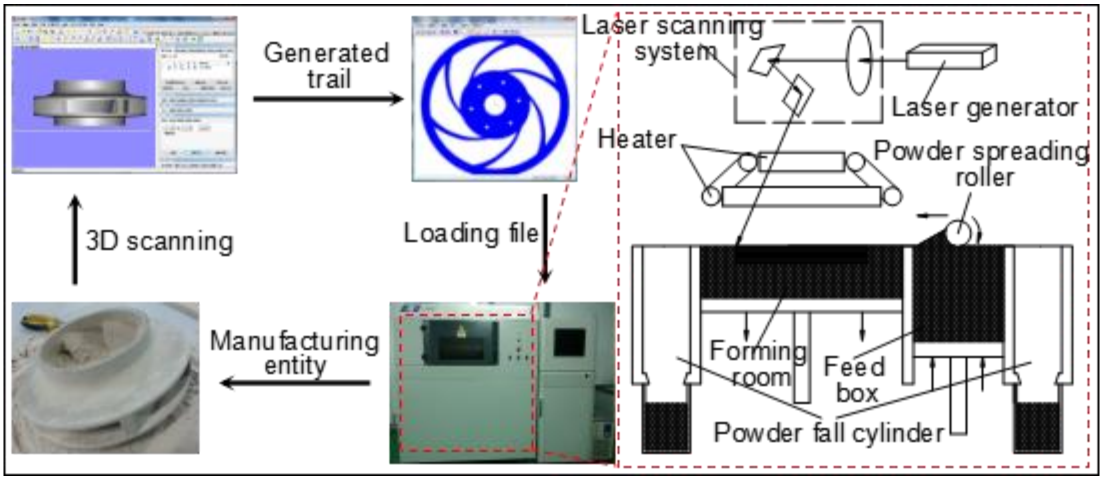

Fig. 1. Rapid prototyping equipment and process schematic diagram

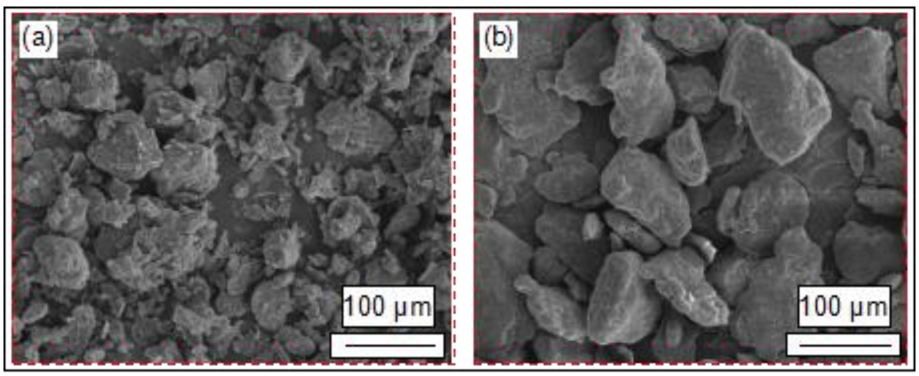

Fig. 2. SEM images of walnut shell powder and Co-PES powder: (a) Walnut shell powder and (b) Co-PES powder

The waste walnut shell was first pulverized into powder with a particle diameter range of 58 μm to 96 μm. The walnut shell powder was then dehydrated for 3.5 h in an incubator (Longyuan Technology Ltd., Beijing, China) at 105 °C. During dehydration, the walnut shell powder was weighed at 1 h intervals until the mass became constant. Then, the dried walnut shell powder was mixed with Co-PES in a 2:3 ratio using a SHR50A high-speed mixer from Hongji Machinery Ltd. (Zhangjiagang, China). To obtain the powder particles of preferable dispersity, the light stabilizers and lubricants were added during the mixing process. The powder was mixed for 15 min below 30 °C at low-speed and then 5 min at high-speed. The mixed powder was taken out from the high-speed mixer and cooled down naturally to obtain the WSPC powder for SLS.

Methods

Orthogonal experiment design

In the SLS process, the density, dimensional precision, and mechanical performance of the WSPC parts are important factors to evaluate the formability. The forming of SLS is a very complicated process. The density, dimensional precision, and mechanical properties mainly depend on the process parameters of the sintered parts. Therefore, an orthogonal experimental design of five factors and four levels was used in the SLS experiment for WSPC powder. The influences of the process parameters of the WSPC parts on density, Z-dimensional precision, and mechanical properties were studied to obtain the forming rules for SLS. The test scheme of WSPC powder in SLS is shown in Table 1.

Table 1. The Factors and Levels of Laser Sintering Test

Levels	Laser Power (W), [A]	Scan Speed (mm/s), [B]	Layer Thickness (mm), [C]	Scan Spacing (mm), [D]	Preheating Temperature (°C), [E]
1	08	1600	0.10	0.10	78
2	10	1800	0.15	0.15	80
3	12	2000	0.20	0.20	82
4	14	2200	0.25	0.25	84

Material characterization and properties test – Scanning electronic microscopy (SEM)

The walnut shell powder and Co-PES powder were scanned using a FEI Quanta200 SEM (Hewlett-Packard Company, Amsterdam, Netherlands). The SEM images of the morphologies of the walnut shell powder and Co-PES powder were obtained (Fig. 2).

Density

The mass and dimensions of the WSPC parts were measured *via* an electronic balance and vernier caliper. Herein, the density ρ is calculated *via* Eq. 1,

$$\rho = \frac{W}{l \cdot b \cdot h} \tag{1}$$

where W denotes the mass of parts (g), l represents the length of parts (mm), b is the width of parts (mm), and h denotes the thickness of parts (mm).

Dimensional precision

A rectangular specimen with dimensions of 80 mm × 10 mm × 4 mm was used in the precision analysis. The WSPC parts were fabricated by SLS according to the different process parameters (Table 1). The actual dimensions of the WSPC parts were measured using a vernier caliper. Herein, the dimensional precision δ is calculated *via* Eq. 2,

$$\delta\,(\%) = (1 - \frac{|L_0 - L|}{L_0}) \tag{2}$$

where δ represents the dimensional precision of parts (%), L_0 denotes the standard dimension of parts (mm), and L indicates the actual dimension of parts (mm). The dimension of WSPC parts in the Z direction (direction of thickness) was also measured, and the Z-dimensional precision δ_z was calculated (%).

Mechanical property

A mechanical property of the WSPC parts was tested using a CMT5504 tensile testing machine from MTS Industrial Systems (China) Co., Ltd. (Shenzhen, China). The testing standard used was ISO 527-2 (1993). The crosshead speed was 5 mm/min and the gauge length was 50 mm.

RESULTS AND DISCUSSION

Single Factor Analysis

The Z-dimensional precision, tensile strength, and density of WSPC parts were determined by the range analysis method, and the obtained range value was used to evaluate the influence of process parameters on the quality of WSPC parts, as shown in Table 2. A larger range value illustrated that the influence of process parameters on the quality of WSPC parts was larger. Table 2 showed that the order of the range value of Z-dimensional precision of WSPC parts from large to small was as follows: scan spacing > laser power > layer thickness > scanning speed > preheating temperature. This result illustrated that the scan spacing had greatest influence on the Z-dimensional precision while the preheating temperature had least influence. Scan spacing had the largest influence on tensile strength while the preheating temperature had least influence on the tensile strength, and layer thickness had greatest influence on density, however, preheating temperature had least influence on density.

Table 2. Range Value of the Influence of Process Parameters on the Quality of WSPC Parts

Test Index	Laser Power (W), [A]	Scan Speed (mm/s), [B]	Layer Thickness (mm), [C]	Scan Spacing (mm), [D]	Preheating Temperature (°C), [E]
Z-dimensional precision (δ_z)	8.100	3.850	4.275	9.750	3.675
Tensile strength (σ_b)	1.072	0.443	1.108	1.781	0.422
Density (ρ)	0.068	0.024	0.084	0.083	0.021

Through an orthogonal experiment, the influences of the process parameters on the Z-dimensional precision of WSPC parts were obtained, as shown in Fig. 3. Figures 3(a) to 3(e) show that with increased laser power, the power absorbed by powder bed increased and the powder was fully fused. The power diffused along the laser-sintering path and the sintered depth was increased, which increased the dimension of sintering parts in the Z-direction and thus, the Z-dimensional precision decreased. Furthermore, with increased preheating temperature, the temperature gradually reached the hardening temperature of powder. Un-sintered powder adhered to the sintered parts and the powder cleaning was difficult, which increased the dimension of sintering parts in the Z-direction, and thus, Z-dimensional precision was decreased. Figures 3(b) and 3(d) show that the power absorbed by the powder-bed decreased with increasing scanning speed. Less power diffused along the laser-sintering path and the sintered depth was decreased, which increased the Z-dimensional precision. With an increase in scan spacing, the re-sintering zone was reduced, and the sintered depth decreased, resulting in an increased Z-dimensional precision. Figure 3(c) shows that when the input power of the laser was kept constant, with decreasing layer thickness, the re-sintered zone increased and the sintered depth increased, and thus the dimension of sintering parts in the Z-direction increased. Thus, Z-dimensional precision decreased. However, when the layer thickness was greater than 0.15 mm, the power absorbed by the powder bed gradually decreased, and the powder was not fully fused, which increased the dimension of sintering parts in the Z-direction. Thus, the Z-dimensional precision again decreased.

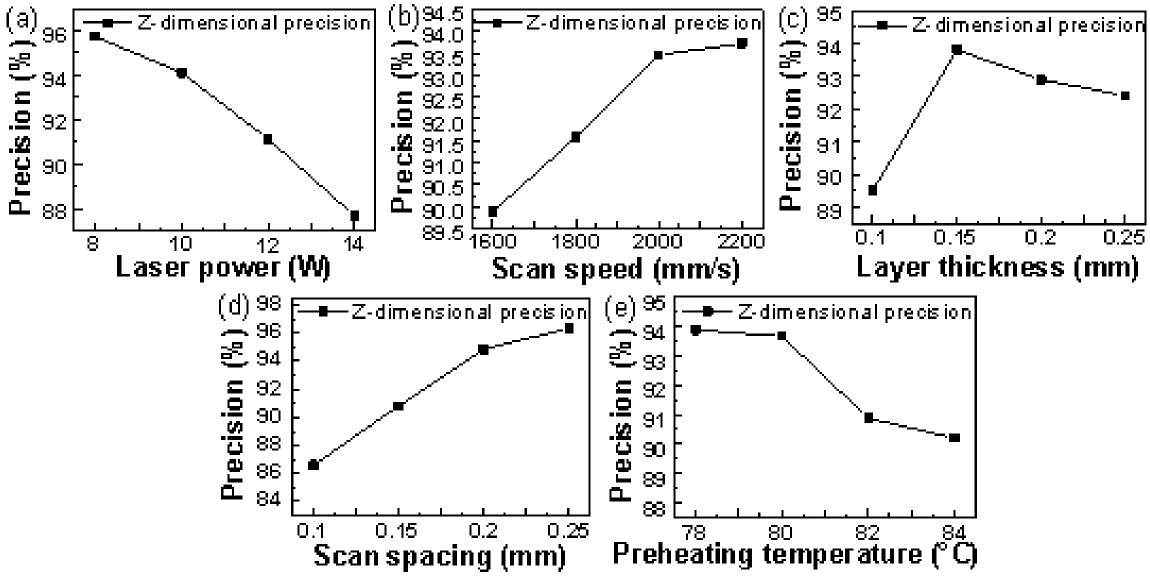

Fig. 3. Influence of process parameters on Z-dimensional precision of WSPC parts: (a) Laser power; (b) Scanning speed; (c) Layer thickness; (d) Scan spacing; and (e) Preheating temperature

As shown in Fig. 4, through an orthogonal experiment, the influence of the process parameters on the tensile strength of WSPC parts was obtained. Figures 4(a) and 4(e) show that with the increase of laser power and preheating temperature, the power absorbed by the powder bed increased and the powder was completely fused. Moreover, the presence of the adhesive and solidification enhanced the interfacial bonding strength between the walnut shell powder and the Co-PES matrix. Thus, the tensile strengths of sintered parts were increased.

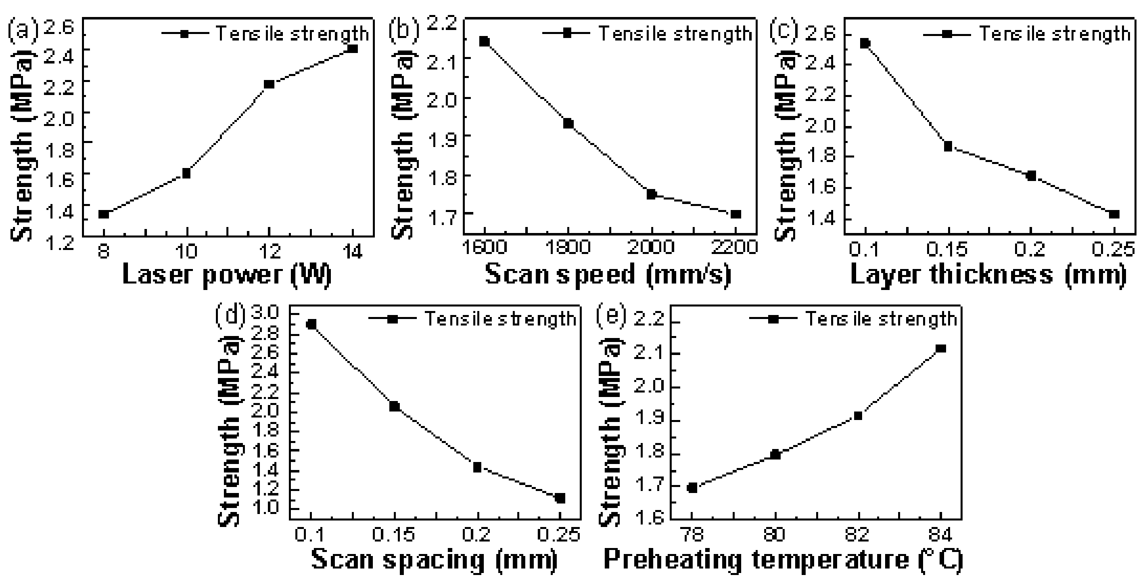

Fig. 4. Influence of process parameters on tensile strength of WSPC parts: (a) Laser power; (b) Scanning speed; (c) Layer thickness; (d) Scan spacing; and (e) Preheating temperature

Figures 4(b) to 4(d) show that when the scanning speed increased, only a shorter time was available for the laser beam to radiate the powder bed. The power absorbed by powder bed decreased and the powder was not fully fused, which decreased the interfacial bonding strength between the walnut shell powder and the Co-PES matrix. Thus, the tensile strengths of sintered parts were decreased. When the input power of laser was kept constant, with an increase of layer thickness, the power absorbed by combination zone between layer and layer was decreased, and the powder was not fully fused, which decreased the interfacial bonding strength between the walnut shell powder and Co-PES matrix. The adhesion property between layer and layer is poor, and layers were separated. Thus, the tensile strength of sintered parts decreased. With increased scan spacing, the re-sintering zone was reduced, the power absorbed by powder bed gradually decreased, and the powder was not fully fused, which decreased the interfacial bonding strength between the walnut shell powder and Co-PES matrix. Thus, the tensile strengths of sintered parts were decreased.

Through an orthogonal experiment, the influence rules of the process parameters on the density of WSPC parts were obtained, as shown in Fig. 5. Figures 5(a) to 5(e) show that with the increase of laser power and preheating temperature, the power absorbed by powder bed increased, the powder was fully fused, and the quantities of internal pores of sintered parts decreased. Thus, the density of sintered parts increased. Figure 5(b) shows that when the scanning speed was slow, a longer time was required for laser beam to radiate the powder bed. When the power absorbed by the powder bed increased, the dimensions in X, Y, and Z directions increased, and correspondingly the volume became bigger. Thus, the densities of sintered parts were decreased. However, when the scanning speed was greater than 1800 mm/s, the power absorbed by powder bed gradually decreased, and amounts of internal pores of sintered parts gradually increased, and the quality of sintered parts also gradually decreased. Thus, the density of sintered parts decreased.

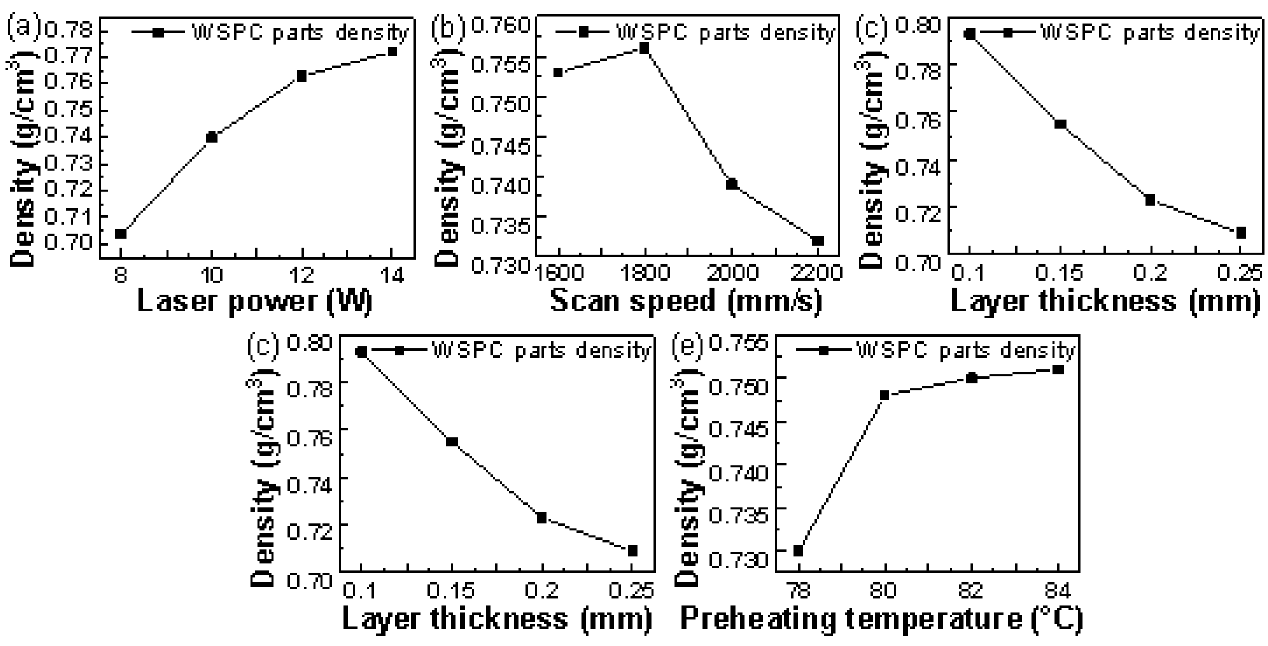

Fig. 5. Influence of process parameters on density of WSPC parts: (a) Laser power; (b) Scanning speed; (c) Layer thickness; (d) Scan spacing; and (e) Preheating temperature

Figures 5(c) and 5(d) show that when the input power of laser was kept constant, with increasing layer thickness, the power absorbed by combination zone between layer and layer was decreased, and the powder was not fully fused. Thus, the quantities of internal pores of sintered parts increased. The density of sintered parts decreased. With the increase of scan spacing, the re-sintering zone was reduced, the power absorbed by the powder bed gradually decreased, the powder was not fully fused, and the amounts of internal pores of sintered parts gradually increased. Thus, the densities of sintered parts were decreased.

Multi-index Synthetic Analysis

Synthetic weighted evaluation

The Z-dimensional precision, tensile strength, and density were the three evaluation indexes considered for this analysis. Multi-index test results were evaluated by the synthetic weighted scoring method. The synthetic weighted scoring method is a method by which the weights of multi-index were determined according to the importance of each test index in the whole test. The test results of multi-index were transformed to the test results of single index, and then the test scheme was optimized according to the single index analysis method.

Dimensionless test index

The Z-dimensional precision, tensile strength, and density were transformed to dimensionless forms. The transformations were performed in accordance to Eqs. 3 to 5:

$$Z_1 = \frac{z_1 - z_{min}}{z_{max} - z_{min}} \tag{3}$$

$$Z_2 = \frac{z_2 - z_{min}}{z_{max} - z_{min}} \tag{4}$$

$$Z_3 = \frac{z_3 - z_{min}}{z_{max} - z_{min}} \tag{5}$$

Synthetic weights of test index

The density and tensile strength of WSPC part were larger indicated the inner structure of part was denser and mechanical property was better. The higher Z-dimensional precision revealed better forming precision. According to the importance of the test indexes, the test indexes were given weights. In general, the index of more subjective importance was given the larger weights and the index of less subjective importance was given smaller weights.

The influences of Z-dimensional precision and tensile strength were the key consideration, and the density was the secondary consideration. The weights of Z-dimensional precision, tensile strength, and density were λ_1 = 0.5, λ_2 = 0.4, and λ_3 = 0.1, respectively. Therefore, the synthetic weighted scoring values are shown by Eq. 6:

$$Z = \lambda_1 Z_1 + \lambda_2 Z_2 + \lambda_3 Z_3 \tag{6}$$

Results and analysis of the test

Test data were processed by the synthetic weighted scoring method. The range analysis results of Z-dimensional precision, tensile strength, and density were obtained, as shown in Table 3.

Table 3. Laser Sintering Process Scheme and Quality Results of Parts

Serial Number	Laser Power (W) [A]	Scan Speed (mm/s) [B]	Layer Thickness (mm) [C]	Scan Spacing (mm) [D]	Preheating Temperature (°C) [E]	Test Index			
						Density (g/cm^3)	Dimensional Precision (%)	Tensile Strength (MPa)	Synthetic Weights
1	8	1600	0.1	0.1	78	0.792	87	3.089	0.604
2	8	1600	0.15	0.15	80	0.742	97	1.474	0.642
3	8	1600	0.2	0.2	82	0.658	99.2	0.604	0.552
4	8	1600	0.25	0.25	84	0.625	99.8	0.179	0.500
5	10	1800	0.15	0.2	84	0.741	94.2	1.658	0.592
6	10	1800	0.1	0.25	82	0.768	93.8	1.587	0.586
7	10	1800	0.25	0.1	80	0.747	91.6	1.956	0.563
8	10	1800	0.2	0.15	78	0.703	96.8	1.220	0.587
9	12	2000	0.2	0.25	80	0.716	95.3	1.389	0.575
10	12	2000	0.25	0.2	78	0.700	95.2	1.154	0.536
11	12	2000	0.1	0.15	84	0.825	86.5	3.119	0.611
12	12	2000	0.15	0.1	82	0.813	87.5	3.040	0.621
13	14	2200	0.25	0.15	82	0.762	83	2.434	0.408
14	14	2200	0.2	0.1	84	0.815	80.3	3.518	0.495
15	14	2200	0.15	0.25	78	0.725	96.5	1.326	0.603
16	14	2200	0.1	0.2	80	0.786	90.8	2.360	0.611
K1	0.575	0.545	0.603	0.571	0.583	Optimum Combination: C2A3E2B3D3			
K2	0.582	0.565	0.615	0.562	0.598				
K3	0.586	0.582	0.552	0.573	0.542				
K4	0.529	0.580	0.502	0.566	0.549				
R	0.057	0.037	0.113	0.011	0.056				

Table 3 shows that the range of C was largest, which had the greatest influence on the test index. Level 2 was suitable for C; the ranges of A and E were similar, which was smaller than that of C, namely, its influence was less than C. Level 3 was suitable for A, and Level 4 was suitable for E; the range of B was smaller than that of A, C, and E, implying their influence was less. Level 3 was suitable for B; the range of D was the smallest, hence the influence was least. Level 3 was suitable for D. Thus, C2A3E2B3D3 was the optimum combination of various factors, namely, the laser power was 12 W, scanning speed was 2000 mm/s, layer thickness was 0.15 mm, scan spacing was 0.2 mm, and preheating temperature was 80 °C. This optimization was designed at improving the Z-dimensional precision, tensile strength, and density of the WSPC parts, which provided a basis for the choice of the process parameters and gave a new direction for subsequent SLS experiment of biomass composite powder.

Contrast analysis of indexes

There were process defects such as warping deformation, layer-separation, and over-sintering of WSPC parts *via* SLS (Figs. 6a to 6c). After the process parameters were optimized, a higher Z-dimensional precision, larger tensile strength, and density of WSPC parts were obtained *via* SLS (Figs. 6d and 6e). Figure 6e shows that the light brown WSPC part had a clear outline, good surface quality, and high shape precision, thus it was often used as a prototype of new product development, which facilitated the structural modification and reduced the development cycle of a new product. It also used as a demonstration to promote product.

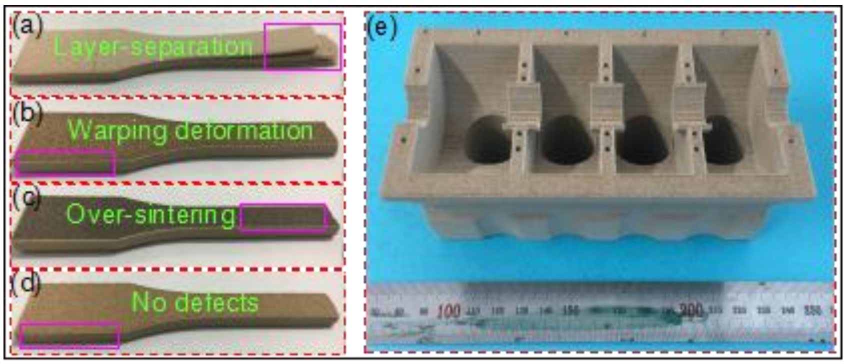

Fig. 6. WSPC parts: (a) No. 4 part; (b) No. 7 part; (c) No. 14 part; (d) No. 4 optimized part; and (e) Engine box

Table 4. Contrast Data of Test Results

Test Contrast	Tensile Strength (MPa)	Z-dimensional Precision (%)	Density (g/cm^3)
Optimized	1.487	97.75	0.743
Optimum	1.474	97	0.742

The optimized process parameters were compared with the optimum combination of synthesis weighted scoring values (Table 3), and the analysis results are shown in Table 4. Table 4 shows that the Z-dimensional precision of WSPC parts increased 0.77% using the optimized process parameters in SLS, compared with that of using optimum combination of synthesis weighted scoring values. As an important index used to evaluate the quality of WSPC parts, the higher Z-dimensional precision indicated better forming precision where the tensile strength increased 0.88%, and a higher tensile strength indicated an improved mechanical property. The density increased 0.13%, which indicated a dense inner structure. The cross-section microstructure of optimized WSPC part is shown in Fig. 7. It can be seen that under processing parameters of SLS, Co-PES powder is fully melted, and a lot of continuous phase form. The surface of cross-section is relatively compact, and there is less porosity. Walnut shell powder particles are evenly distributed in the Co-PES matrix, and fully wrapped by Co-PES, thus, interface bonding effect between them is good. Therefore, the Z-dimensional precision, tensile strength, and density of WSPC parts were improved by the optimized process parameters, and thus the quality of WSPC parts was improved.

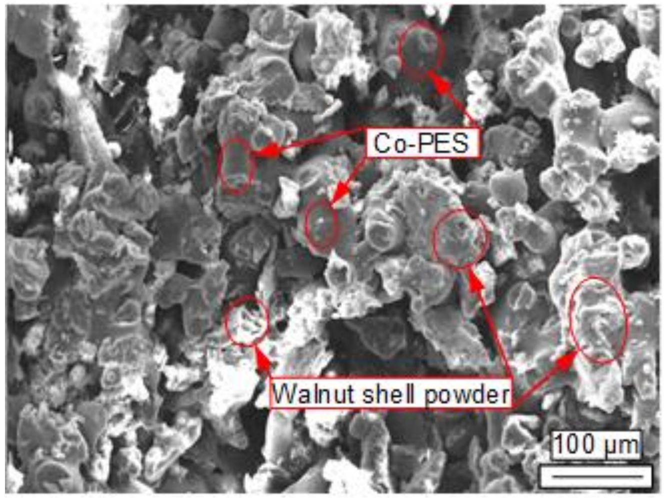

Fig. 7. SEM figure of cross-section of WSPC part

CONCLUSIONS

1. The Z-dimensional precision, tensile strength, and density of WSPC parts were assessed by the range analysis method, and the obtained range value was used to evaluate the influence of process parameters on the quality of WSPC parts. Scan spacing had greatest influence on Z-dimensional precision and tensile strength, and layer thickness had greatest influence on density of WSPC parts. However, preheating temperature had least influence on Z-dimensional precision, tensile strength, and density of WSPC parts.
2. Through an orthogonal experiment of five factors and four levels, the influence of the process parameters on WSPC parts was as follows from large to small: layer thickness > laser power > preheating temperature > scanning speed > scan spacing. The optimum combination was C2A3E2B3D3 of various factors, namely, laser power was 12 W, scanning speed was 2000 mm/s, layer thickness was 0.15 mm, scan spacing was 0.2 mm, and preheating temperature was 80 ℃
3. The Z-dimensional precision of WSPC parts increased 0.77% using the optimized process parameters in SLS. Upon comparison, using the optimum combination of synthesis weighted scoring values, the tensile strength increased 0.88%, and the density increased 0.13%. The optimized process parameters ensured the high quality of WSPC parts fabricated by SLS and provided a reference value for the choice of process parameters of biomass composite of SLS.

ACKNOWLEDGMENTS

This study was supported by the National Natural Science Foundation of China (51475089), the National Key R&D Program of China (2017YFD0601004), the Fundamental Research Funds for the Central Universities (2572017BB07), the 'Double First-Class' Fund of Northeast Forestry University (41112448), the Innovation Funds of the Central University (2572015AB12), the Outstanding Academic Leaders Funds of

Harbin (2015RAXXJ022), and the Special Project of Scientific and Technological Development of Central Guidance for Local (ZY16C03).

REFERENCES CITED

Bai, J., Zhang, B., Song, J., Bi, G. J., Wang, P., and Wei, J. (2016). "The influence of treatment conditions on the mechanical properties of polyethylene produced by selective laser sintering," *Polymer Testing* 52, 89-93. DOI: 10.1016/j.polymertesting.2016.04.004

Deckard, C. R. (1988). *Selective Laser Sintering*, Ph.D. Dissertation, University of Texas at Austin, Austin, TX, USA.

Guo, Y. L., Jiang, K. Y., Yu, Z. X., Xin, Z. S., and Zeng, W. L. (2011). "The preparation technology and forming properties of biomass composite powder used in selective laser sintering," *Journal of Shanghai Jiaotong University* 45(9), 1327-1331.

ISO 527-2 (1993). "Plastics-Determination of tensile properties – Part 2: Test conditions for moulding and extrusion plastics," International Organization for Standardization, Geneva, Switzerland.

Jia, L. B., Wang, X. C., Wang, X. J., Xu, B., and Wei, J. (2015). "The research and application progress of selected laser sintering technology," *Information Technology & Informatization* 11, 172-175. DOI: 10.3969/j.issn.1672-9528.2015.11.054

Mangano, F., Bazzoli, M., Tettamanti, L., Farronato, D., Maineri, M., Macchi, A., and Mangano, C. (2013). "Custom-made, selective laser sintering (SLS) blade implants as a non-conventional solution for the prosthetic rehabilitation of extremely atrophied posterior mandible," *Lasers in Medical Science* 28(5), 1241-1247. DOI: 10.1007/s10103-012-1205-1

Pace, M. L., Guarnaccio, A., Dolce, P., Mollica, D., Parisi, G. P., Lettino, A., Medici, L., Summa, V., Ciancio, R., and Santagata, A. (2017). "3D additive manufactured 316L components microstructural features and changes induced by working life cycles," *Applied Surface Science* 418(1), 437-445. DOI: 10.1016/j.apsusc.2017.01.308

Qi, F. W., Chen, N., and Wang, Q. (2017). "Preparation of PA11/$BaTiO_3$, nanocomposite powders with improved processability, dielectric and piezoelectric properties for use in selective laser sintering," *Materials & Design* 131, 135-143. DOI: 10.1016/j.matdes.2017.06.012

Stašić, J., Trtica, M., Rajković, V., Ružić, J., and Božić, D. (2014). "Laser sintering of Cu-Zr-$ZrBr_2$ composite," *Applied Surface Science* 321, 353-357. DOI: 10.1016/j.apsusc.2014.10.021

Warnakula, A., and Singamneni, S. (2017). "Selective laser sintering of nano Al_2O_3 infused polyamide," *Materials* 10(8), 864. DOI: 10.3390/ma10080864

Yu, Y. Q., Guo, Y. L., Jiang, T., Jiang, K. Y., and Guo, S. (2017). "Laser sintering and post-processing of a walnut shell/Co-PES composite," *RSC Advances* 7(37), 23176-23181. DOI: 10.1039/c7ra00775b

Zeng, W. L., Guo, Y. L., Jiang, K. Y., Yu, Z. X., and Liu, Y. (2012a). "Preparation and selective laser sintering of rice husk-plastic composite powder and post treatment," *Digest Journal of Nanomaterials and Biostructures* 7(3), 1063-1070.

Zeng, W. L., Guo, Y. L., Jiang, K. Y., Yu, Z. X., Liu, Y., Shen, Y. D., Deng, J. R., and Wang, P. X. (2012b). "Laser intensity influence on mechanical properties of wood–

plastic composite parts fabricated by selective laser sintering," *Journal of Thermoplastic Composite Materials* 26(1), 125-136. DOI: 10.1177/0892705712461520

Zhang, H., Guo, Y. L., Zhao, D. J., and Yu, Z. X. (2014). "Preparation and selective laser sintering of pine/polyether sulfone composite," *Journal of Northeast Forestry University* 42(11), 150-152, and 157. DOI: 10.3969/j.issn.1000-5382.2014.11.034

Zhao, D. J., Guo, Y. L., Song, W. L., and Jiang, K. Y. (2015a). "Preparation and forming characteristics of bamboo powder/co-polyamide laser sintering composite materials," *Journal of Northeast Forestry University* 43(6), 107-109, and 115. DOI: 10.13759/j.cnki.dlxb.2015.06.003

Zhao, J. L., Sun, J. W., Ou, B. F., Jiang, L. L., and Pei, T. (2015b). "Application of selective laser sintering technology in injection mould," *Die & Mould Industry* 41(10), 1-4. DOI: 10.16787/j.cnki.1001-2168.dmi.2015.10.001

Zheng, Z. F., Zou, J. C., Hua, B., Zhang, H. J., and Wang, R. (2006). "Study on the constituents of walnut shell," *J. Southwest Forestry College* 26(2), 33-36. DOI: DOI:10.3969/j.issn.2095-1914.2006.02.008

Article submitted: December 4, 2017; Peer review completed: February 17, 2018; Revised version received and accepted: Feburary 28, 2018; Published: March 6, 2018.
DOI: 10.15376/biores.13.2.3017-3029